Impaired hemoglobin clearance by sinusoidal endothelium promotes vaso-occlusion and liver injury in sickle cell disease

Tomasz W. Kaminski,[1*°] Omika Katoch,[1*°] Ziming Li,[1] Corrine B. Hanway,[1] Rikesh K. Dubey,[1°] Adekunle Alagbe,[1] Tomasz Brzoska,[1] Hong Zhang,[2] Prithu Sundd,[1,3,4°] Gregory J. Kato,[5] Enrico M. Novelli[1,6] and Tirthadipa Pradhan-Sundd[1,6°]

[1]Pittsburgh Heart, Lung and Blood Vascular Medicine Institute, University of Pittsburgh School of Medicine, Pittsburgh, PA; [2]BioMagis Inc., San Diego, CA; [3]Department of Bioengineering, University of Pittsburgh, Pittsburgh, PA; [4]Division of Pulmonary Allergy and Critical Care Medicine, Department of Medicine, University of Pittsburgh School of Medicine, Pittsburgh, PA and [5]CSL Behring, King of Prussia, PA and [6]Division of Hematology/Oncology, Department of Medicine, University of Pittsburgh School of Medicine, Pittsburgh, PA, USA

**TWK and OK contributed equally as first authors.*
°Current address: Versiti Blood Research Institute and Medical College of Wisconsin, Milwaukee, WI, USA

Correspondence: Tirthadipa Pradhan-Sundd
tip9@pitt.edu
tpradhan@versiti.org

Received: June 21, 2023.
Accepted: November 2, 2023.
Early view: November 9, 2023.

https://doi.org/10.3324/haematol.2023.283792

Abstract

Sickle cell disease (SCD) is a monogenic disorder that affects 100,000 African-Americans and millions of people worldwide. Intra-erythrocytic polymerization of sickle hemoglobin (HbS) promotes erythrocyte sickling, impaired rheology, ischemia and hemolysis, leading to the development of progressive liver injury in SCD. Liver-resident macrophages and monocytes are known to enable the clearance of HbS; however, the role of liver sinusoidal endothelial cells (LSEC) in HbS clearance and liver injury in SCD remains unknown. Using real-time intravital (*in vivo*) imaging in mice liver as well as flow cytometric analysis and confocal imaging of primary human LSEC, we show for the first time that liver injury in SCD is associated with accumulation of HbS and iron in the LSEC, leading to senescence of these cells. Hemoglobin uptake by LSEC was mediated by micropinocytosis. Hepatic monocytes were observed to attenuate LSEC senescence by accelerating HbS clearance in the liver of SCD mice; however, this protection was impaired in P-selectin-deficient SCD mice secondary to reduced monocyte recruitment in the liver. These findings are the first to suggest that LSEC contribute to HbS clearance and HbS-induced LSEC senescence promotes progressive liver injury in SCD mice. Our results provide a novel insight into the pathogenesis of hemolysis-induced chronic liver injury in SCD caused by LSEC senescence. Identifying the regulators of LSEC-mediated HbS clearance may lead to new therapies to prevent the progression of liver injury in SCD.

Introduction

Sickle cell disease (SCD) is an autosomal recessive genetic disorder that affects approximately 100,000 Americans and millions of people worldwide.[1] A point mutation in the β-globin gene (β6Glu→Val) promotes intra-erythrocytic hemoglobin-S (HbS) polymerization in SCD, leading to erythrocyte dehydration, increased membrane stiffness with a characteristic sickle-shape, and hemolysis.[1] As a result of altered morphology and impaired rheology of sickle erythrocytes, patients with SCD experience several clinical complications, such as acute systemic painful vaso-occlusive episodes, acute chest syndrome, stroke, and chronic organ damage,[2-5] which contribute to a significantly reduced life expectancy and quality of life.[6,7]

Sickle red blood cells are prematurely cleared from the circulation by reticulo-endothelial macrophages.[8-10] Recent evidence suggests that liver sinusoidal endothelial cells (LSEC) support the tethering of damaged erythrocytes to hepatic sinusoids, leading to sequestration and subsequent clearance of these cells by intraluminal liver macrophages (Küpffer cells).[11,12] Using quantitative liver intravital microscopy (qLIM),[12] as well as flow cytometric analysis and confocal imaging of primary human and mouse LSEC, we show for the first time that

chronic liver injury in SCD mice is associated with micropinocytosis-mediated uptake of HbS in the LSEC, leading to LSEC senescence. We also show that LSEC senescence is enhanced in the absence of tissue-resident leukocytes (as seen in P-selectin-deficient SCD mice) due to increased intake of HbS resulting in exacerbated liver injury. Our results reveal novel insights into the hepatic hemoglobin clearance pathway as well as the pathogenesis of hemolysis-driven chronic liver injury caused by HbS-induced LSEC senescence in SCD.

Methods

Animals

Townes SCD mice (SS, homozygous for *Hba*$^{tm1(HBA)Tow}$, homozygous for *Hbb*$^{tm2(HBG1,HBB*)Tow}$) and non-sickle control (AS) mice (AS, homozygous for *Hba*$^{tm1(HBA)Tow}$, compound heterozygous for *Hbb*$^{tm2(HBG1,HBB*)Tow}$/*Hbb*$^{tm3(HBG1,HBB)Tow}$)[14] were obtained from Jackson Laboratories (Bar Harbor, ME, USA) and housed in a specific pathogen-free animal facility at the University of Pittsburgh (Pittsburgh, PA, USA). Littermate AS mice have been used widely as control mice in several prior studies focused on SCD pathophysiology.[15-17] Littermate Townes AS and SCD mice were used as the control and SCD mice, respectively, in all experiments. Townes SCD mice were bred to Selp$^{-/-}$ mice to generate P-selectin-deficient SCD (SCD; Selp$^{-/-}$) mice using the breeding strategy described by Bennewitz *et al.*[18] All animal experiments were approved by the Institutional Animal Care and Use Committee at the University of Pittsburgh. Five or more mice were assessed at all given timepoints.

Analysis of liver biopsies from patients with sickle cell disease

This study was approved by the local Institutional Review Board (University of Pittsburgh) and conducted in accordance with the Declaration of Helsinki and National Institutes of Health guidelines for using human specimens. De-identified needle biopsy specimens of liver from SCD patients and age-matched healthy control humans were retrospectively reviewed for associated pathology and liver disease. Samples were obtained for light microscopy using standard procedures.[19]

Human and mice primary liver sinusoidal endothelial cell cultures

Human primary endothelial cells were obtained from iXCell Biotechnology (San Diego, CA, USA). LSEC were cultured with endothelial cell growth medium (iXCell Biotechnology) based on the vendor's protocol. Mouse primary endothelial cells (C57BL/6 Mouse Liver Sinusoidal Endothelial Cells) were obtained from Accegen (Fairfield, NJ, USA).

Flow cytometry

Human or murine LSEC were treated with 2 μM of fluorescein isothiocyanate-tagged hemoglobin (Sigma, Carlsbad, CA, USA) or ferrous stabilized human HbS protein (Sigma) by adding the stimulus in the culture media. The cells were then detached by 0.25% trypsin (Sigma) followed by one wash. The surfaces of the detached cells were stained with Alexa 647 CD31 (Abcam, Waltham, Boston, USA) or phycoerythrin-CD31 (BioLegend, San Diego, CA, USA), and calcium-free apoptotic-dead cell tag 488 (BioMagis, San Diego, CA, USA catalog n. 302104) or calcium-free apoptotic-dead cell tag Atto 647 (BioMegis) for 15 minutes at room temperature in the dark followed by one wash. Next the cells were stained with iFluor 647 Anti-Hb Rabbit pAb antibody (BioMegis) at room temperature in the dark after fixation with 4% paraformaldehyde and permeabilization by 0.25% Triton X-100. The cells were analyzed with a NovoCyte Penteon flow cytometer (Beckman). The data shown were gated on live cells.

Blocking micropinocytosis and endocytosis in primary liver sinusoidal endothelial cells

To block micropinocytosis we used nystatin (50 μg/mL) for about 30 minutes, as described elsewhere.[20] Cells were exposed to latrunculin A (0.24 mM/L) for 2 hours to block endocytosis.[21]

Statistical analysis

All comparisons between two groups were deemed statistically significant if the *P* value of an unpaired two-tailed Student *t* test was less than 0.05 (**P*<0.05; ***P*<0.01).

Further information

Additional methods used in this study are standard and are described in the *Online Supplementary Supporting Information*. *Online Supplementary Tables S1, S2* and *S3* summarize the antibodies used for immunohistochemistry, western blotting, and intravital imaging, respectively. *Online Supplementary Table S4* lists the primers employed in this study, while *Online Supplementary Table S5* presents the cell culture reagents used in the *in vitro* assays.

Results

Liver sinusoidal endothelial cells exhibit senescence in mice with sickle cell disease

Previously, we showed that SCD mice manifest liver senescence and hepatobiliary injury under baseline conditions.[19] To further confirm the type of liver cell undergoing senescence, we used multiphoton excitation which enabled *in vivo* real-time fluorescence microscopy of the intact liver in live mice (Figure 1A). The method of qLIM is described elsewhere.[22] Texas red-dextran and AF488-P21 antibodies (*Online Supplementary Table S3*) were administered intravascularly to visualize the blood flow in liver sinusoids and identify senescent cells in SCD (SS) and control (AS) mice, respectively (Figure 1A, upper panel; *Online Supplementary*

Movies S1 and *S2*). As shown in Figure 1A, P21-positive cells were localized close to the hepatic sinusoids resembling endothelial cell structures, suggestive of endothelial cell senescence. In contrast, control (AS) mice did not show accumulation of P21-positive senescent cells close to the liver sinusoids (Figure 1A, upper panel; *Online Supplementary Movies S3* and *S4*). Moreover, staining with the endothelial cell marker CD31 and cell senescence marker P21 showed significant co-localization in the SCD mice liver compared to that in control mice liver (Figure 1B, quantified in *Online Supplementary Figure S1A*).

As endothelial cells are the predominant non-hepatocyte cell type in the liver,[23] we analyzed the mRNA and protein expression of markers of senescence in non-hepatocytes isolated from the liver[24] of control and SCD mice. As shown in Figure 1C, non-hepatocytes from SCD mice had significantly higher expression of senescence markers, detected by quantitative real-time polymerase chain reaction (qRT-PCR) (P21, P16 and P53 expression) (*Online Supplementary Table S4*) and demonstrated by western blot (P53 and P21 expression). When examined by transmission electron micrography, LSEC from SCD mice contained dark inclusions (which are detected in senescent cells as signs of DNA damage), which were not present in LSEC from control (AS) mice (Figure 1D). Finally, immunohistochemistry staining revealed greater accumulation of SA-β-galactosidase

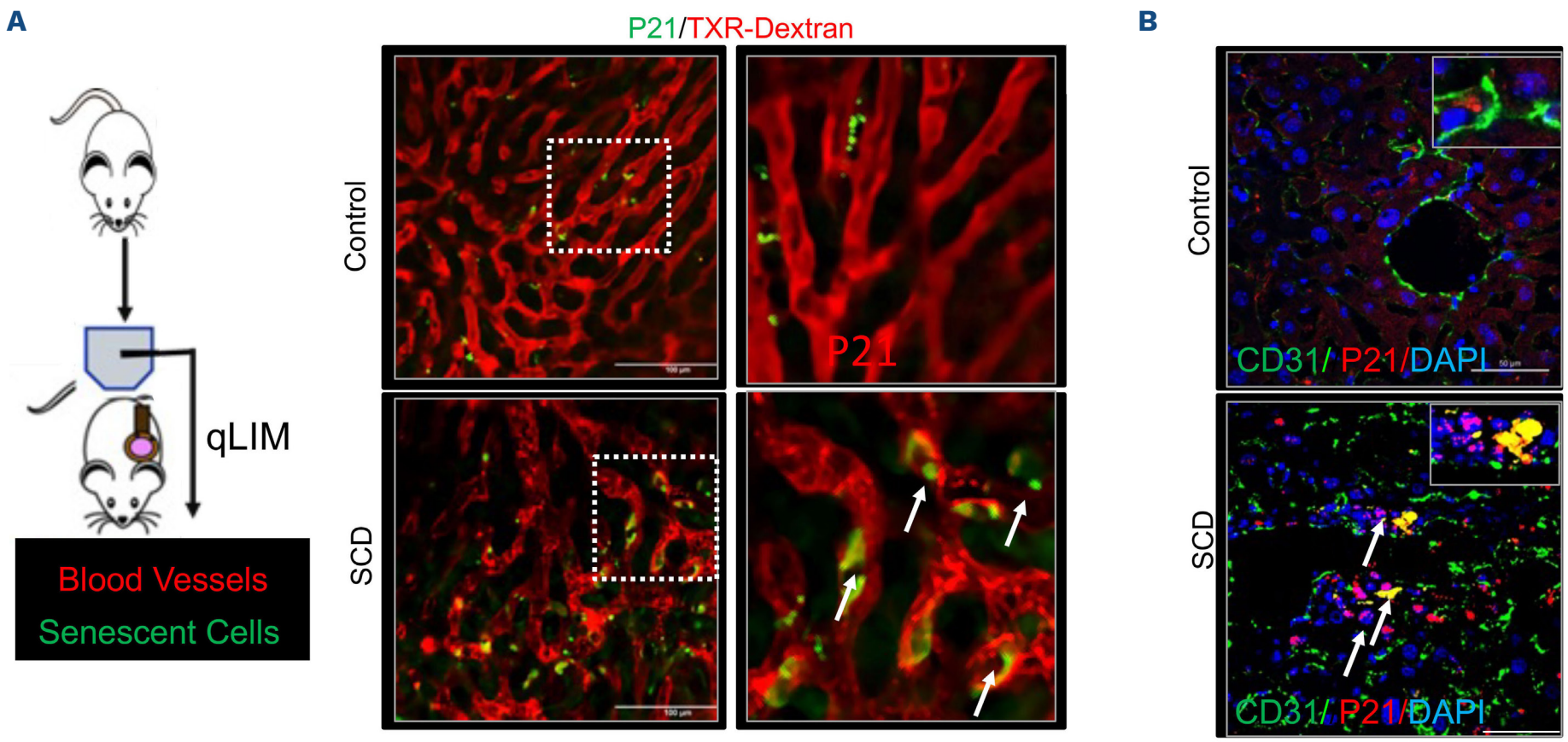

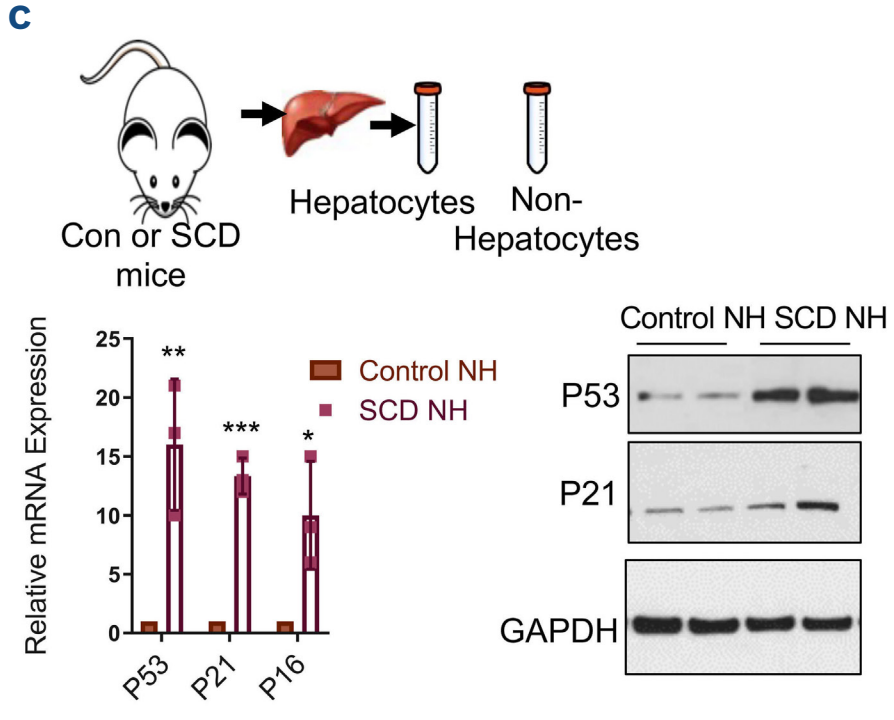

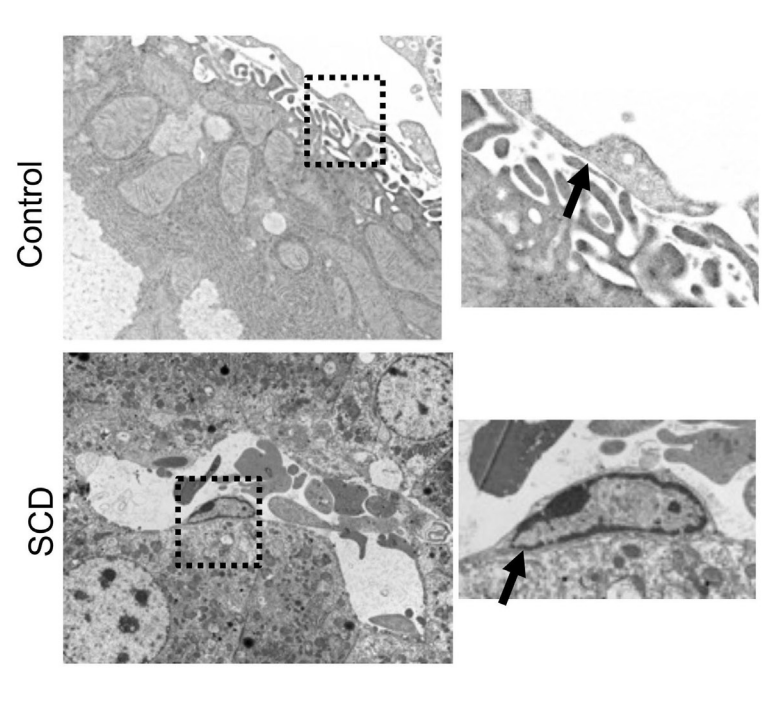

Continued on following page.

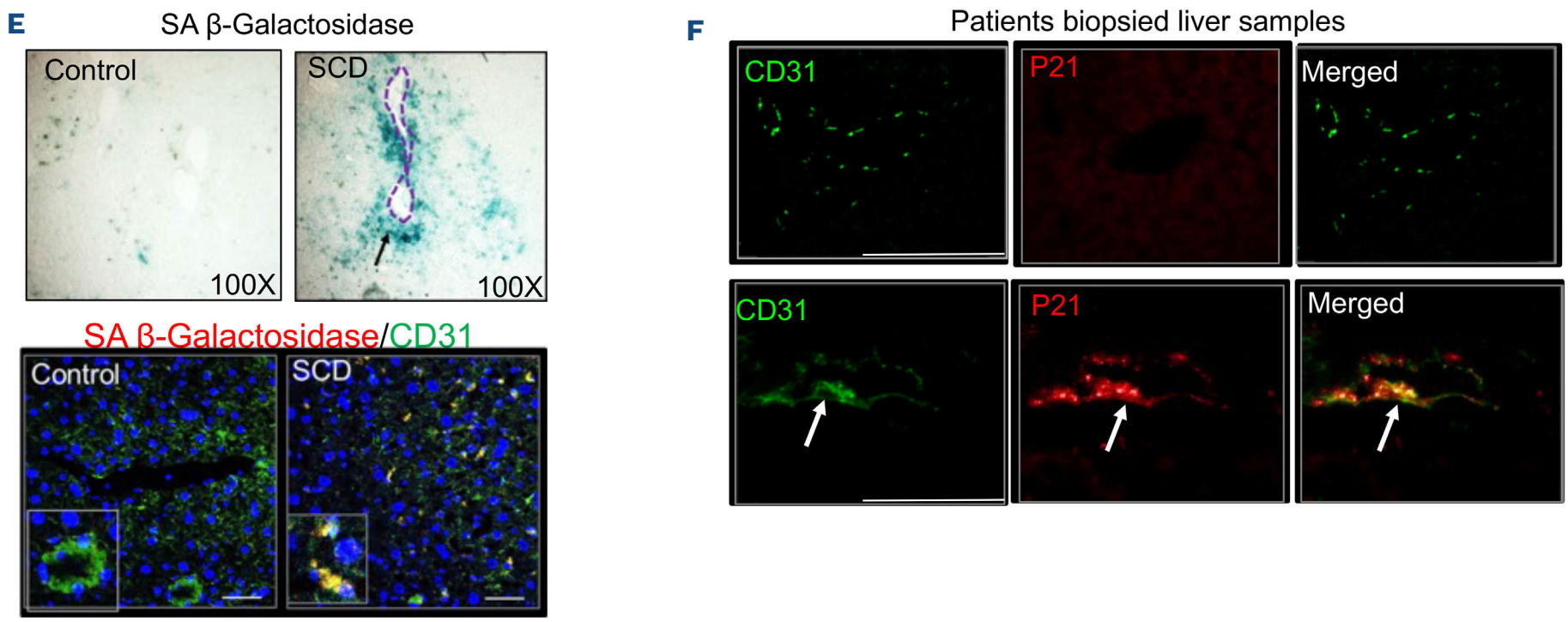

Figure 1. Liver sinusoidal endothelial cells exhibit senescence in sickle cell disease liver. (A) Schematic diagram of quantitative liver intravital microscopy (qLIM) imaging of mice using Texas Red-dextran and AF488-P21 antibody. Representative qLIM images of sickle cell disease (SCD) liver injected with Texas Red-dextran and AF488-P21 antibody. The arrows indicate the presence of P21 in endothelial cell-like structures. The images on the right are zoomed in views of the areas in the dotted boxes. (B) Representative immunofluorescent images of P21 reveal significant co-localization with CD31 in SCD mouse liver compared to that in control mouse liver. (C) Schematic diagram of non-hepatocyte isolation from control and SCD mouse liver. The lower left panel shows quantitative real-time polymerase chain reaction analysis of control and SCD mouse liver, demonstrating increased expression of senescent markers P53, P21 and P16 in SCD non-hepatocytes as compared with control non-hepatocytes. *P<0.05 **P=0.05 and ***P=0.01. The lower right panel shows a western blot for P53 and P21 antibodies, demonstrating increased expression in SCD non-hepatocytes compared with the expression in control non-hepatocytes. (D) Representative transmission electron micrographs of control and SCD mouse livers showing the presence of electron-dense liver sinusoidal endothelial cells (LSEC) in SCD liver which was not seen in control liver tissue. (E) The upper panels are representative images of SA-β-galactosidase staining in control and SCD liver tissue (the dotted circle marks a portal triad of liver which surrounds LSEC). The lower panels are representative images of control and SCD mouse liver tissue showing co-localization of SA-β-galactosidase with the LSEC marker CD31. (F) Representative images of liver biopsies from age-matched control human and SCD patients showing enhanced co-localization of P21 with the LSEC marker CD31 in SCD patients. Scale bar 50 μm. DAPI: 4',6-diamidino-2-phenylindole; Con: control; NH: non-hepatocytes; GAPDH: glyceraldehyde-3-phosphate dehydrogenase.

(a marker of senescence) around LSEC in SCD mice liver than in control (AS) mice liver (Figure 1E, upper panel). This was further validated by increased co-localization of the endothelial cell marker CD31 and cell senescence marker SA-β galactosidase in the liver of SCD mice as compared to control mice liver (Figure 1E, lower panel). Finally, we also found significant co-localization of the cell senescence marker P21 and endothelial cell marker CD31 in biopsied liver tissue sections from SCD patients compared to that in healthy human liver tissue sections (Figure 1F). Taken together, these data suggest that LSEC undergo senescence in both SCD mice and SCD patients' biopsied liver tissue sections.

Liver sinusoidal endothelial cell senescence in sickle cell disease mice is associated with hepatic sequestration of red blood cells and accumulation of hemoglobin-heme-iron in the endothelial cells

Next, we explored whether LSEC senescence is caused by increased red blood cell sequestration in the hepatic sinusoids. Scanning electron micrography revealed the presence of a significantly higher number of erythrocytes in SCD hepatic sinusoids than in control (AS) liver sinusoids (Figure 2A, upper panel; *Online Supplementary Figure S1B*), suggestive of hepato-sinusoidal erythrocyte retention/red blood cell sequestration. Damaged erythrocytes can release hemoglobin, which is cleared in the liver by tissue-resident Küpffer cells[10] and monocyte-derived macrophages.[25] Recent studies have also suggested a possible role for endothelial cells in hemoglobin clearance.[10,26,27] We hypothesized that entrapped sickled erythrocytes are hemolyzed in the hepatic sinusoids to release hemoglobin, which is internalized by both LSEC and Küpffer cells/monocytes in the liver. Western blot analysis showed significantly greater accumulation of hemoglobin in the SCD mouse liver tissue than in control (AS) mouse liver (Figure 2A, lower panel). We next examined hemoglobin localization in SCD liver using a fluorescent tagged normal hemoglobin antibody, Hb-AF647. As shown in Figure 2C, hemoglobin localized mostly to Küpffer cells in the control liver. In a few cases, LSEC-specific localization of hemoglobin was also seen, suggesting a role of LSEC in hemoglobin clearance. Remarkably, hemoglobin localization was significantly enhanced in Küpffer cells as well as in LSEC in SCD mice liver compared to that in control (AS)

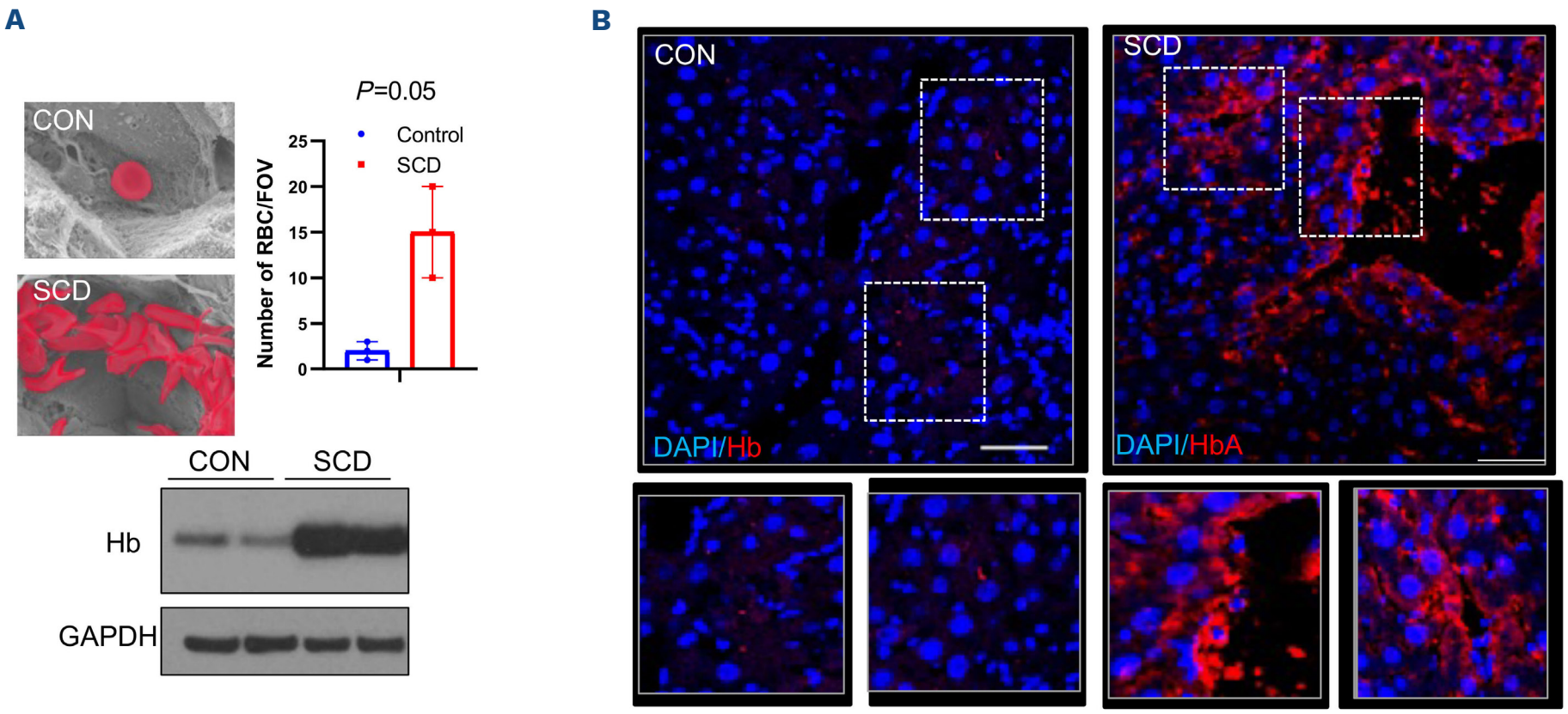

Continued on following page.

Figure 2. Liver sinusoidal endothelial cell senescence is associated with prolonged retention of sickled erythrocytes in hepatic sinusoids and accumulation of hemoglobin in the liver sinusoidal endothelial cells. (A) Upper panel: representative scanning electron micrographs showing entrapment of erythrocytes in liver sinusoids of sickle cell disease (SCD mice compared to that in control mice, quantified in the bar graph to the right. Lower panel: western blot analysis showing increased expression of hemoglobin in SCD mouse liver compared to that in control mouse liver. (B) Representative immunofluorescence images of hemoglobin-AF647 showing enhanced expression of hemoglobin in SCD mouse liver compared to control mouse liver. Hemoglobin expression was also enriched in liver sinusoidal endothelial cells (LSEC) of SCD mice. Zoomed images of the dotted regions are shown below. (C) Representative immunofluorescence images show strong co-localization of hemoglobin with the LSEC marker CD31 and Küpffer cell marker CLEC4F in SCD liver. (D) Representative immunohistochemistry images of Perls Prussian blue staining show accumulation of iron in LSEC (arrow) of SCD liver at baseline which was not seen in control liver. (E) Schematic showing the experimental design to examine hemoglobin trafficking in SCD liver. Representative immunofluorescence images for hemoglobin-AF647 reveal increased expression of hemoglobin in LSEC of SCD mice at 8 hours after injection which was not seen in control (AS) mice liver. (F) Representative immunofluorescence images showing co-localization of hemoglobin and CD31 in SCD liver tissue, which further confirms increased hemoglobin in the LSEC of SCD liver. Scale bar 50 μm. CON: control; RBC: red blood cells; FOV: field of view; Hb: hemoglobin; DAPI: 4',6-diamidino-2-phenylindole; hrs: hours; PI: post-injection.

mice liver (Figure 2C). Additionally, we found significantly greater co-localization of AF647-anti-hemoglobin antibody with the Küpffer cell marker CLEC4F and LSEC marker CD31 (*Online Supplementary Table S1*) in SCD compared to control (AS) mice liver (Figure 2C; *Online Supplementary Figure S1C*).

Further supporting increased uptake of HbS in SCD liver, when we examined hepatic iron accumulation, we could see that along with hepatocytes and Küpffer cells, LSEC were also positive for iron staining in SCD mice liver (Figure 2D, arrow). Finally, we examined whether hemoglobin clearance in the liver of SCD mice is delayed due to LSEC senescence. We injected hemoglobin tagged with AF647 via a tail vein and evaluated the amount of tagged hemoglobin in SCD and control mice liver 8 hours after the injection (Figure 2E). In control mice liver tissue, we found very few AF647-tagged hemoglobin puncta 8 hours after the injection (Figure 2E). However, we found greater accumulation of hemoglobin in the LSEC of SCD mice liver, which is suggestive of delayed hemoglobin clearance (Figure 2F). Collectively, our data suggest that LSEC senescence is associated with sinusoidal erythrocyte retention and increased hemoglobin and iron accumulation in LSEC of SCD mice.

Micropinocytosis promotes hemoglobin uptake by liver sinusoidal endothelial cells

To further characterize LSEC-mediated hemoglobin uptake, we assessed hemoglobin accumulation *in vitro* in cultured primary LSEC. Flow cytometry analysis was applied to evaluate hemoglobin binding to human primary LSEC, using CD31 as a marker for LSEC and hemoglobin/HbS (*Online Supplementary Table S5*) as markers for hemoglobin (Figure 3A). Interestingly, we found strong co-localization of hemoglobin and HbS with CD31 (Figure 3A) in primary human LSEC, confirming the uptake of hemoglobin/HbS by LSEC. As LSEC had not previously been linked to hemoglobin scavenging, we performed additional image analysis to confirm the internalization of hemoglobin by primary LSEC. Figure 3B shows that, with time, hemoglobin accumulation increased in LSEC, confirming hemoglobin uptake. To quantify the percentage of hemoglobin bound or not bound to LSEC, hemoglobin was added to a suspension of LSEC, and the number of hemoglobin-positive cells was determined after 0-30 minutes of incubation. As shown in Figure 3B, we found strong enhancement of hemoglobin staining in LSEC with time. Confocal imaging also showed hemoglobin localization within CD31-positive primary LSEC after the administration of hemoglobin (*Online Supplementary Figure S1D*). Additionally, to assess whether other cell types may also take up hemoglobin or whether this is an LSEC-specific process, we tested the capacity of human lung microvascular endothelial cells to bind hemoglobin. Flow cytometric analysis (*Online Supplementary Figure S1E*, upper panel) as well as confocal imaging (*Online Supplementary Figure S1E*, lower panel) revealed that human primary lung endothelial cells could also take up hemoglobin.

Next, we examined the potential mechanism by which LSEC internalize hemoglobin. Endothelial cells are known to take up diverse biomolecules via the process of micropinocytosis.[28] Thus, we first blocked micropinocytosis using nystatin in a human liver endothelial cell line. Blocking micropinocytosis[29] with nystatin significantly decreased hemoglobin and CD31 co-localization in primary human LSEC (Figure 3C; *Online Supplementary Figure S1F*). Since micropinocytosis is defined as receptor-mediated endocytosis of molecules into a cell,[29] we used latrunculin-A to inhibit endocytosis[30] in human LSEC. Interestingly, latrunculin-A also inhibited the uptake of hemoglobin by LSEC (Figure 3D, *Online Supplementary Figure S1F*). However, compared to nystatin, latrunculin-A was not as effective at blocking hemoglobin internalization (*Online Supplementary Figure S1F*). Taken together, our data suggest that micropinocytosis is the mechanism by which human LSEC internalize hemoglobin.

Accumulation of HbS and iron induces liver sinusoidal endothelial cell senescence

As LSEC senescence in SCD is associated with the accumulation of HbS/iron in LSEC, we hypothesized that senescence of these cells in the SCD liver could also be induced by the accumulation of sickle Hb/iron in LSEC. To examine the effect of iron in promoting LSEC senescence, we administered SCD mice a low dose of iron dextran intra-

A

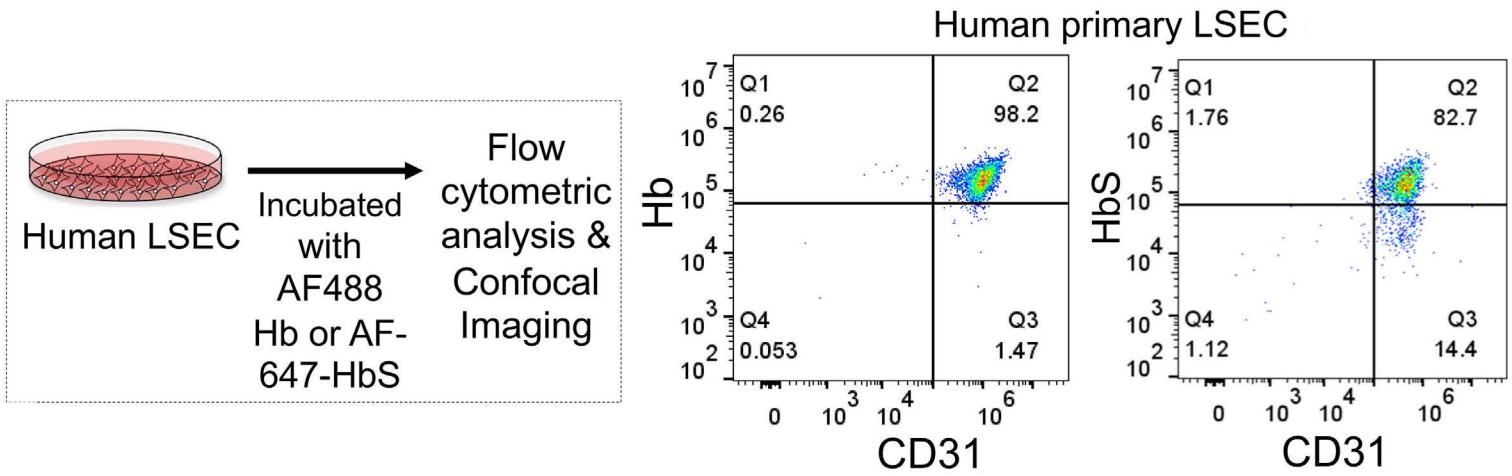

B

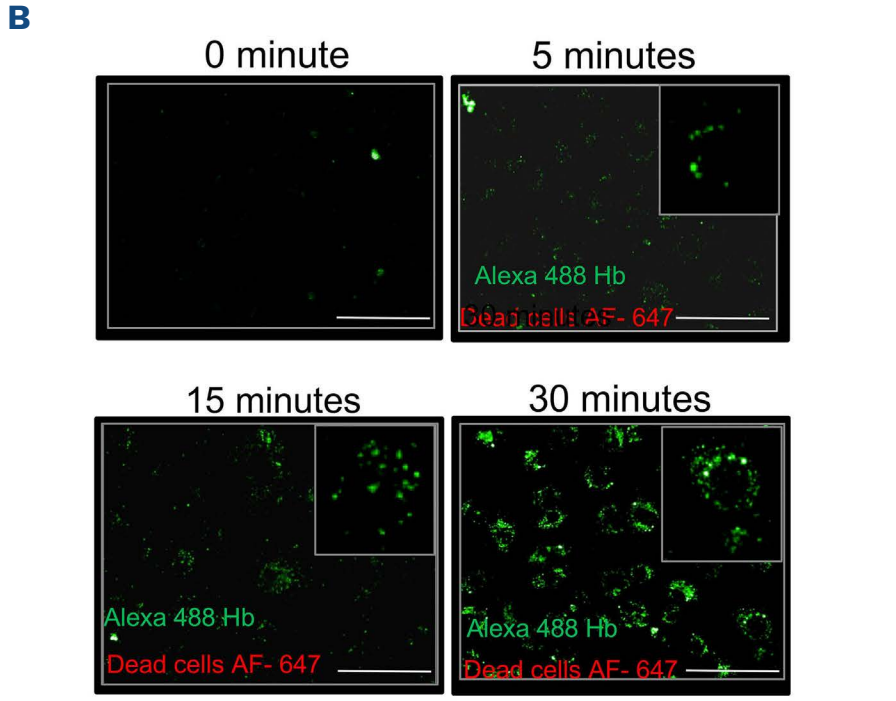

C

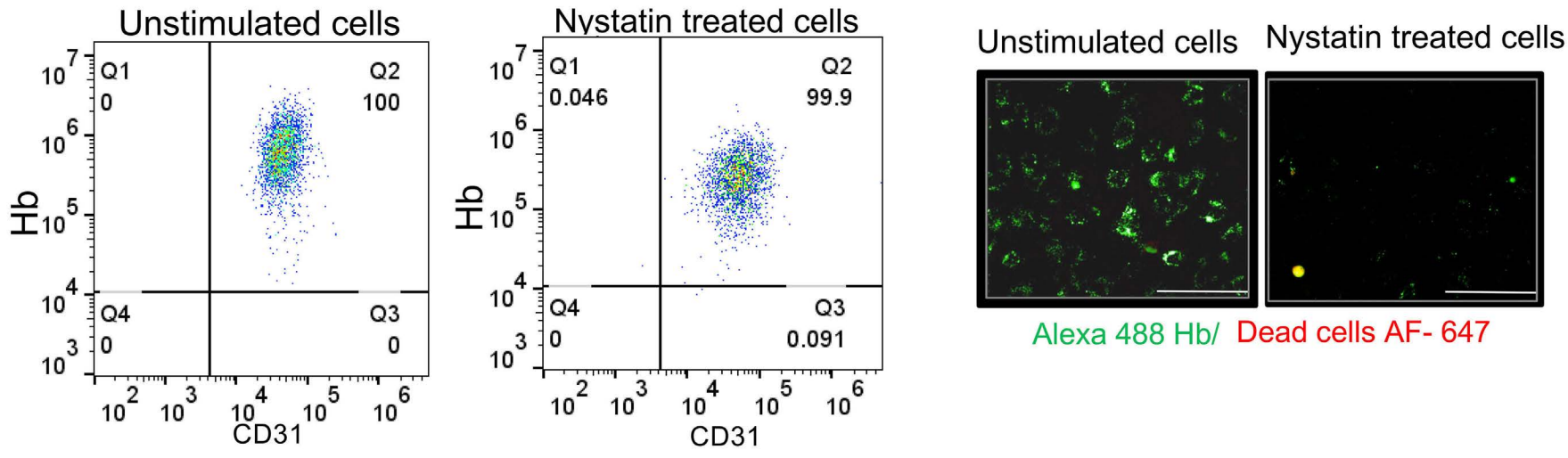

D

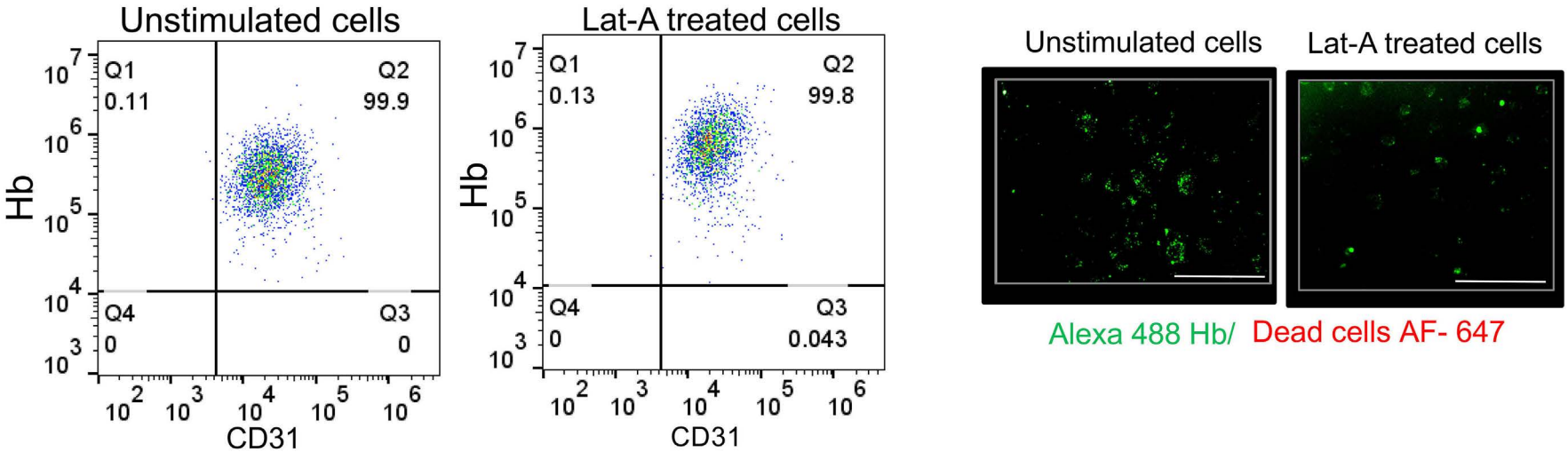

Continued on following page.

Figure 3. *In-vitro* characterization reveals that micropinocytosis is the predominant mechanism of human liver sinusoidal endothelial cell-mediated hemoglobin intake. (A) Schematic diagram of the experimental design for flow cytometry of human primary liver endothelial cells. The right panel shows the flow cytometry analysis of CD31, normal hemoglobin and HbS in human primary liver endothelial cells. (B) Left panel: representative immunofluorescence images showing hemoglobin intake by primary human liver sinusoidal endothelial cells (LSEC) at 0, 5, 15 and 30 minutes after hemoglobin administration. The insets show zoomed in images. Right panel: a bar graph of the percentages of hemoglobin-positive LSEC at different time points. (C) Left panel: flow cytometry analysis of CD31 and hemoglobin in human primary liver endothelial cells with or without nystatin stimulation. Right panel: representative immunofluorescence images of hemoglobin intake by primary human LSEC with or without nystatin stimulation. (D) Left panel: flow cytometry analysis of CD31 and hemoglobin in human primary liver endothelial cells with or without latrunculin-A stimulation. Right panel: representative immunofluorescence images of hemoglobin intake by primary human LSEC with or without latrunculin-A stimulation. *P<0.05. Hb: hemoglobin; Lat-A: latrunculin-A.

peritoneally for up to 3 weeks (Figure 4A). Iron dextran administration increased the level of hepatic iron in SCD mice liver, as seen by western blot for the iron storage protein ferritin (Figure 4A, middle panel) and Perls Prussian blue staining for iron (Figure 4A, right panel). We found strong enrichment of iron in LSEC after iron dextran treatment (Figure 4A, endothelial cells surround the red dotted area). qRT-PCR (Figure 4B, left panel) and western blot analysis (Figure 4B, middle panel; *Online Supplementary Table S2*) for markers of senescence revealed a significant increase in LSEC senescence in the liver of iron dextran-treated SCD mice compared to that in untreated SCD mice. Additionally, exogenous iron exacerbated LSEC senescence based on the finding of increased co-localization of the LSEC marker CD31 and senescence marker P21 in iron dextran-treated *versus* untreated SCD mice (Figure 4B, right panel). Finally, iron dextran significantly increased the serum levels of markers of liver injury (alanine and aspartate transaminases) compared to those in untreated SCD mice (*Online Supplementary Figure S2A*) and resulted in exacerbated endothelial injury which correlated with the accumulation of iron in LSEC detected by staining with Prussian blue (*Online Supplementary Figure S2B*).

To assess the effect of HbS in promoting LSEC senescence, we treated primary human LSEC with normal hemoglobin and with HbS for up to 1 hour (Figure 4C). Interestingly, LSEC showed significant apoptosis after 1 hour of HbS treatment (Figure 4C, D; *Online Supplementary Figure S2C*), which was not observed after hemoglobin treatment. As hemoglobin auto-oxidation and subsequent heme release are more rapid from HbS than from HbA,[31] we hypothesized that once internalized, HbS is more rapidly broken down to heme and iron, causing increased oxidative stress. To confirm our hypothesis, we performed qRT-PCR and analyzed the expression of markers of oxidative stress (NAD[P]H quinone dehydrogenase, glutathione peroxidase 1, superoxide dismutase and glutathione S transferase mu), senescence (P21 and P53), and iron overload (ferritin) following HbA and HbS internalization by LSEC. Remarkably, as shown in Figure 4E and *Online Supplementary Figure S2D*, HbS administration caused an increase in the expression of oxidative stress markers, senescence markers and ferritin as compared to HbA treatment. In addition, we used confocal imaging to examine the fluorescence intensity of HbS and HbA after internalization. As shown in *Online Supplementary Figure S2E*, HbS intensity waned more rapidly over time compared to HbA intensity, indicating a faster rate of degradation of HbS following internalization. Overall, these findings indicate that HbS/iron build-up accelerates LSEC senescence in SCD. Furthermore, these results demonstrate a potential difference in the degradation rates of HbS and HbA within LSEC.

Absence of hepatic leukocytes exacerbates the senescence of liver sinusoidal endothelial cells in sickle cell disease

Liver-resident leukocytes (monocytes, Küpffer cells, and monocyte-derived [transient] macrophages) are the primary cells known to be responsible for hemoglobin clearance in the liver.[32] Previously we[19] and others[33] showed increased expression of leukocytes (monocytes and macrophages) in SCD mouse liver, a phenomenon significantly reduced in SCD mice following P-selectin deletion (SCD; Selp$^{-/-}$ mice).[34] Interestingly, we have also found that chronic P-selectin deficiency in SCD mice exacerbates overall liver senescence and injury.[34] Thus, we hypothesized that the increased liver damage seen in SCD; Selp$^{-/-}$ mice is most likely due to enhanced LSEC senescence. To confirm increased LSEC senescence in SCD; Selp$^{-/-}$ mice, we used qLIM in live animals. As shown in Figure 5A, AF488-P21 antibody staining was strongly enriched in SCD; Selp$^{-/-}$ mouse liver compared to SCD mouse liver (*Online Supplementary Movies S5* and *S6*). Moreover, the endothelial cell marker CD31 co-localized strongly with the cell senescent marker P21 in SCD; Selp$^{-/-}$ liver compared to SCD mouse liver (Figure 5B; *Online Supplementary Figure S3A*). P-selectin deficiency also led to an increase in hemoglobin (Figure 5C, D) and iron accumulation (Figure 5E) within LSEC of SCD mice, which was evidenced by the greater co-localization of hemoglobin than in untreated SCD mice (Figure 5C, upper panel) with the endothelial cell marker CD31 (Figure 5D; *Online Supplementary Figure S3B*). Immunofluorescence of the monocyte marker CD11b showed reduced expression in SCD; Selp$^{-/-}$ mouse liver as compared to that in SCD mouse liver (*Online Supplementary Figure S3C*). Recent evidence suggests that stressed erythrophagocytosis (as seen in hemolytic disorders) results in massive leukocyte infiltration in the liver, predominantly by monocytes that convert

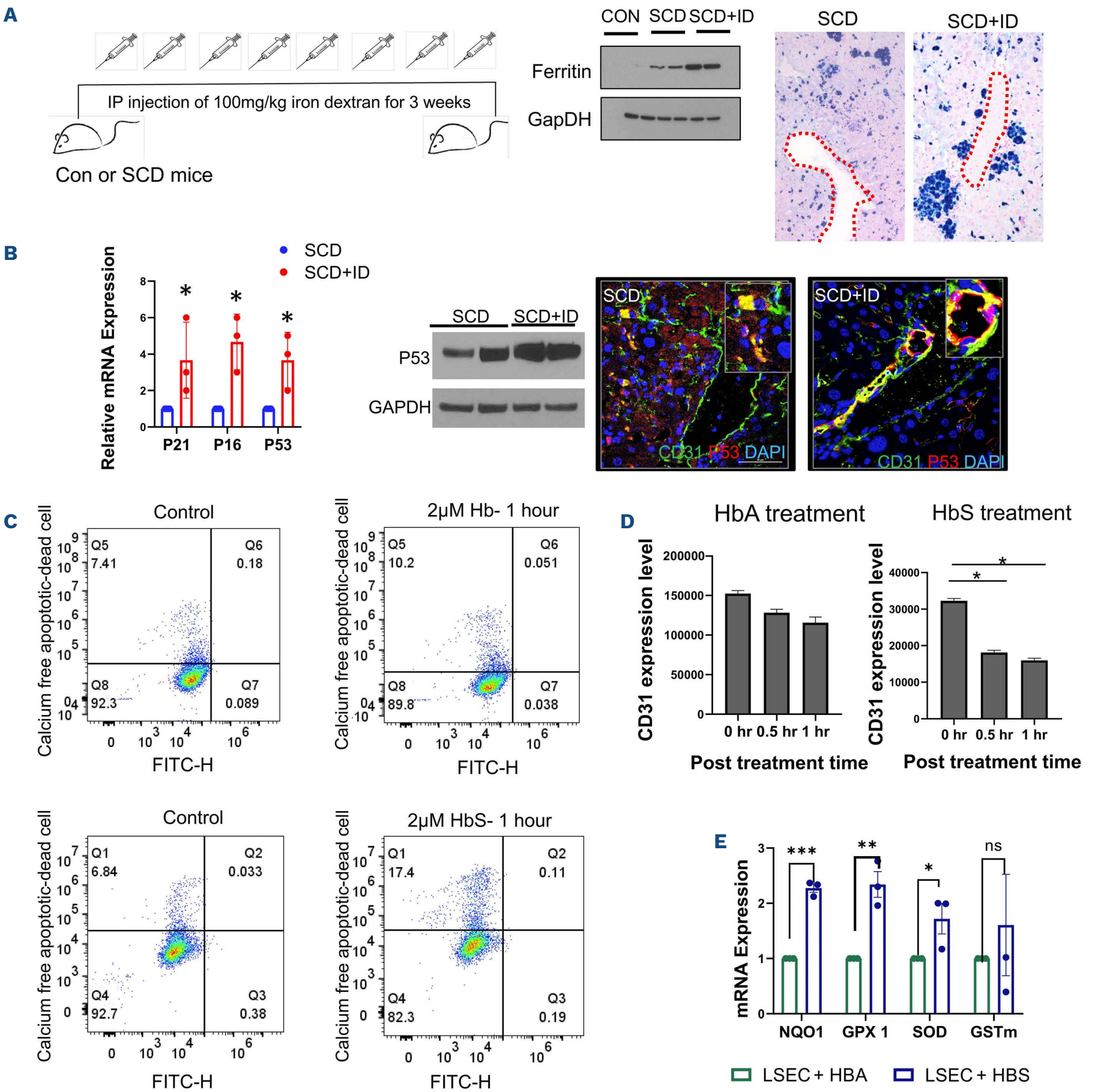

Figure 4. Accumulation of hemoglobin/iron in liver sinusoidal endothelial cells predominantly drives senescence in sickle cell disease liver. (A) Left panel: schematic of iron dextran administration to control and sickle cell disease (SCD) mice. Middle panel: western blot analysis of ferritin showing increased expression after iron dextran treatment in SCD mouse liver compared to control and SCD mouse liver at baseline. Right panel: representative immunohistochemistry images of Perls Prussian blue staining show accumulation of iron in liver sinusoidal endothelial cells (LSEC) of SCD mice at baseline; the accumulation was further increased in iron dextran-treated SCD mice. (B) Left panel: quantitative real-time polymerase chain reaction (qRT-PCR) analysis of P21, P16 and P53 showing increased expression of these markers in SCD liver after iron dextran treatment. Middle panel: western blot analysis of P53 showing increased expression in SCD liver after iron dextran treatment. Right panel: representative immunofluorescence images exhibiting stronger co-localization of P53 with CD31 in SCD liver after iron dextran treatment than at baseline. (C) Flow cytometry analysis of dead cells at baseline and 1 hour after hemoglobin and HbS treatment in primary human LSEC. (D) Bar graphs showing CD31 expression at baseline and 0.5 and 1 hours after HbS treatment. (E) qRT-PCR analysis of markers of oxidative stress in LSEC showing increased expression after HbS treatment compared to that after HbA treatment. **P*<0.05; ***P*=0.05; ****P*=0.01. Scale bar 50 μm. Con: control; IP: intraperitoneal; GAPDH: glyceraldehyde-3-phosphate dehydrogenase; ID: iron dextran; DAPI: 4',6-diamidino-2-phenylindole; FITC-H: fluorescein isothiocyanate pulse height; Hb: hemoglobin; hr: hour; NQO1: NAD(P)H quinone dehydrogenase; GPX 1: glutathione peroxidase 1; SOX: superoxide dismutase; GSTm: glutathione S transferase mu.

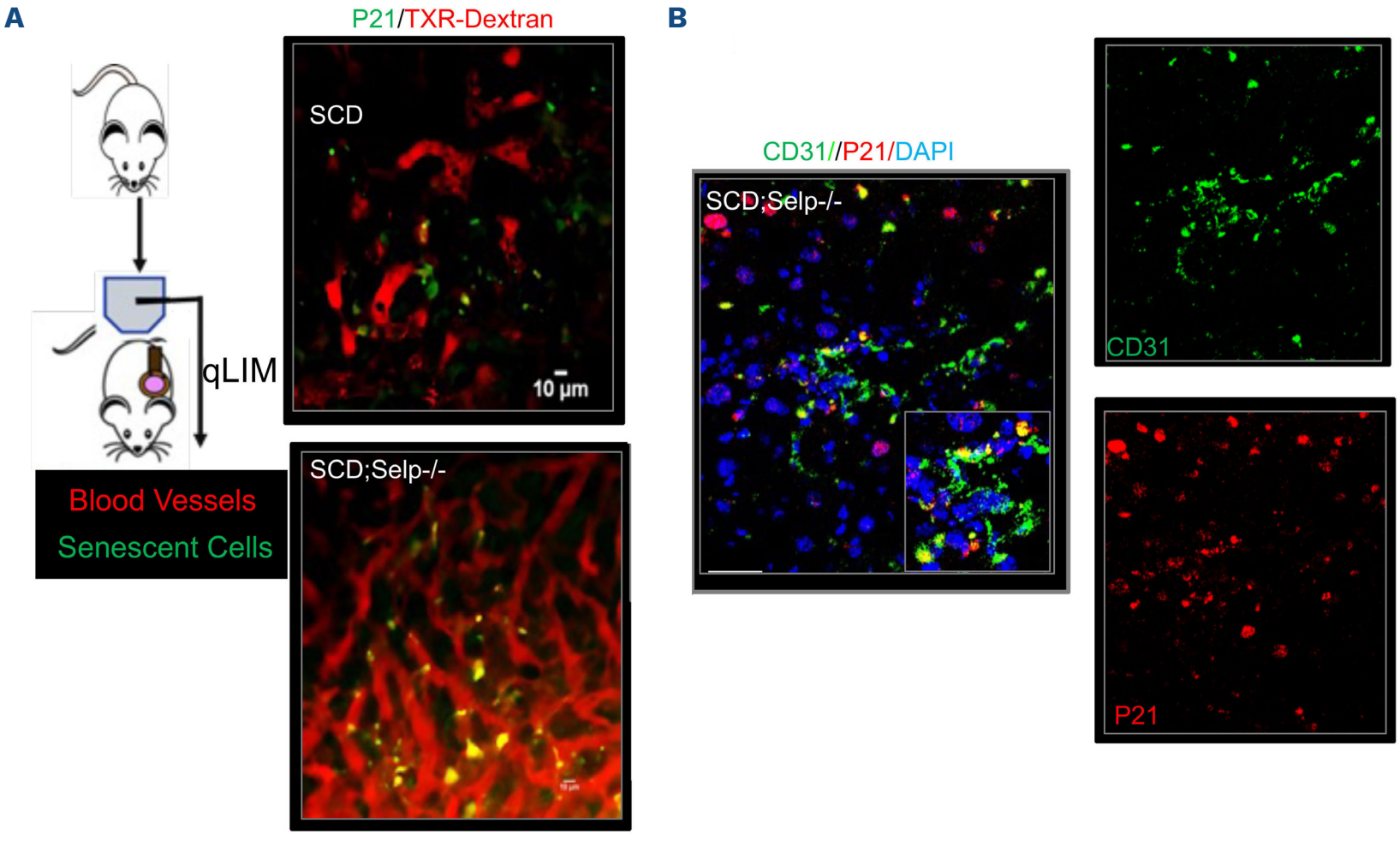

Figure 5. P-selectin-depleted mice with sickle cell disease show exacerbated liver sinusoidal endothelial cell senescence due to impaired hemoglobin clearance. (A) Schematic diagram of quantitative liver intravital microscopy (qLIM) imaging of mice using Texas red-dextran and AF488-P21 antibody. Representative qLIM images of liver tissue from sickle cell disease (SCD) mice and P-selectin-deficient SCD; Selp$^{-/-}$ mice injected with Texas red-dextran and AF488-P21 antibody. (B) Immunofluorescence image of P21 exhibits strong co-localization with CD31 in SCD; Selp$^{-/-}$ mouse liver. (C) Representative immunofluorescence images showing double staining of hemoglobin and CD31 in SCD and SCD; Selp$^{-/-}$ liver. Zoomed in images of the dotted box are shown. (D) Scatter plot showing the co-localized distribution pattern of CD31 (green) and hemoglobin (red) in SCD and SCD; Selp$^{-/-}$ mouse liver. (E) Representative immunohistochemistry images for Perls Prussian blue staining show accumulation of iron in liver sinusoidal endothelial cells of SCD mouse liver at baseline, which is enhanced in SCD; Selp$^{-/-}$ mouse liver. Scale bar 50 µm. TXR: Texas red; DAPI: 4',6-diamidino-2-phenylindole; Hb: hemoglobin.

into tissue-resident macrophages (also known as monocyte-derived macrophages).[25] As we saw significant loss of monocytes in SCD; Selp$^{-/-}$ mice, we hypothesized that LSEC senescence is directly linked to loss of hepatic monocytes and monocyte-derived macrophages. To test this hypothesis, we sought to deplete monocytes and macrophages from SCD mouse liver. In order to selectively deplete monocytes, we used a low dose of clodronate liposome (10% of the normal dose), as previously described.[35,36] As expected, we observed a strong reduction of the monocyte marker CD11b in the liver after clodronate liposome treatment (Figure 6A). Interestingly, we found that the depletion of hepatic monocytes in SCD mice by clodronate liposomes led to an increase in the total number of erythrocytes sequestered in hepatic sinusoids, as shown by scanning electron micrography (Figure 6B; *Online Supplementary Figure S3D*), which was associated with exacerbated liver senescence, evidenced by increased mRNA (Figure 6C, left panel) and protein expression (Figure 6C, middle panel) of markers of senescence. Loss of hepatic monocytes also led to increased co-localization of CD31 and P53 (Figure 6C, right panel) as well as an increase in hemoglobin accumulation, as shown by the higher level of hemoglobin than in untreated SCD mice (Figure 6D) and the greater co-localization of hemoglobin with the endothelial cell marker CD31 (Figure 6D; *Online Supplementary Figure S3E*).

We hypothesized that exacerbated LSEC senescence can promote vaso-occlusion and damage-associated molecular pattern (DAMP)-associated chronic liver injury. As we found more pronounced LSEC senescence in clodronate-treated SCD mouse liver, we analyzed liver injury in these animals compared to that in untreated SCD mice. We found a significant increase in serum alanine aminotransferase and aspartate transaminase in clodronate-treated SCD mice as compared to that in untreated SCD mice, which is indicative of exacerbated liver injury in clodronate-treated SCD mice (*Online Supplementary Figure. S3F*). Furthermore, sinusoidal congestion and increased liver injury were more pronounced in clodronate-treated SCD mice than in untreated ones, as shown by staining hepatic tissue with hematoxylin and eosin (Figure 6E). Sirius red and α-smooth muscle actin (α-SMA) staining (Figure 6E) revealed more collagen deposition and activated myofibroblasts in the clodronate-treated SCD mouse livers than in untreated ones, suggesting more severe liver fibrosis in the clodronate-treated animals. As shown by qLIM (Figure 6F), SCD mice manifested loss of blood flow in several regions of the liver at baseline due to sinusoidal vaso-occlusion.[19] Following treatment with clodronate liposomes, SCD mice showed a further increase in areas with vaso-occlusion (Figure 6F; *Online Supplementary Figure S4A*, *Online Supplementary Movies S7* and *S8*). Depletion of hepatic Küpffer cells (*Online Supplementary Figure S4B*) also resulted in similar enhancement of hepatic senescence (*Online Supplementary Figure S4C, D*) and exacerbated liver injury (*Online Supplementary Figure S4E*). Collectively, our data suggest that exacerbated LSEC senescence and delayed HbS/red blood cell clearance are associated with increased vaso-occlusion, tissue damage and elevated levels of liver enzymes in monocyte-depleted SCD mice.

Discussion

Sickle red blood cells are prematurely cleared from the circulation by reticulo-endothelial macrophages.[8-10] This process occurs primarily in the spleen until age-induced splenic dysfunction develops,[37] which eventually results in the liver and bone marrow becoming the primary sites for hemoglobin clearance. In the liver, tissue-resident Küpffer cells as well as monocyte-derived macrophages promote hemoglobin clearance.[38] Cell-free HbS released following intravascular hemolysis in SCD is scavenged by plasma haptoglobin, which chaperones it to the liver for CD163-dependent clearance by macrophages.[39] However, chronic hemolysis in SCD results in depletion of plasma haptoglobin, leading to HbS clearance in the liver through a relatively less efficient process involving direct binding of hemoglobin to CD163 on macrophages.[12,40,41] Cell-free hemoglobin released following intravascular hemolysis in SCD is also known to promote endothelial dysfunction in diverse organs by scavenging nitric oxide, promoting the generation of reactive oxygen species, and activating toll like receptor-4-dependent upregulation of pro-inflammatory and prothrombotic adhesion molecules on the surface of endothelial cells.[42-44] Remarkably, our current study is the first to show that LSEC also contribute to the clearance of hemoglobin through micropinocytosis and that internalization of hemoglobin and iron leads to LSEC senescence. Cellular senescence is a state of irreversible growth arrest, which can be induced by a stress response to diverse cellular stimuli.[45] LSEC senescence, a relatively novel concept, was recently found to be associated with sepsis and inflammatory liver diseases.[46] However, the mechanism driving LSEC senescence remains poorly understood. Previous studies proposed that the senescent phenotype is a consequence of de-differentiation or loss of phenotype.[47] Based on the data presented herein, we propose that intracellular accumulation of HbS and its rapid degradation are inducers of LSEC senescence. Prior research has demonstrated that hemoglobin auto-oxidation and subsequent heme release occur more rapidly from sickle hemoglobin (HbS) than from HbA,[31] which could indicate rapid degradation of HbS after its internalization. Our findings also demonstrated increased oxidative stress and iron accumulation after HbS treatment, indicating a fast breakdown of HbS or alterations in its structure after internalization. Additionally, the potential for HbS to undergo polymerization *in vitro* upon internalization is worth considering and requires further investigation.

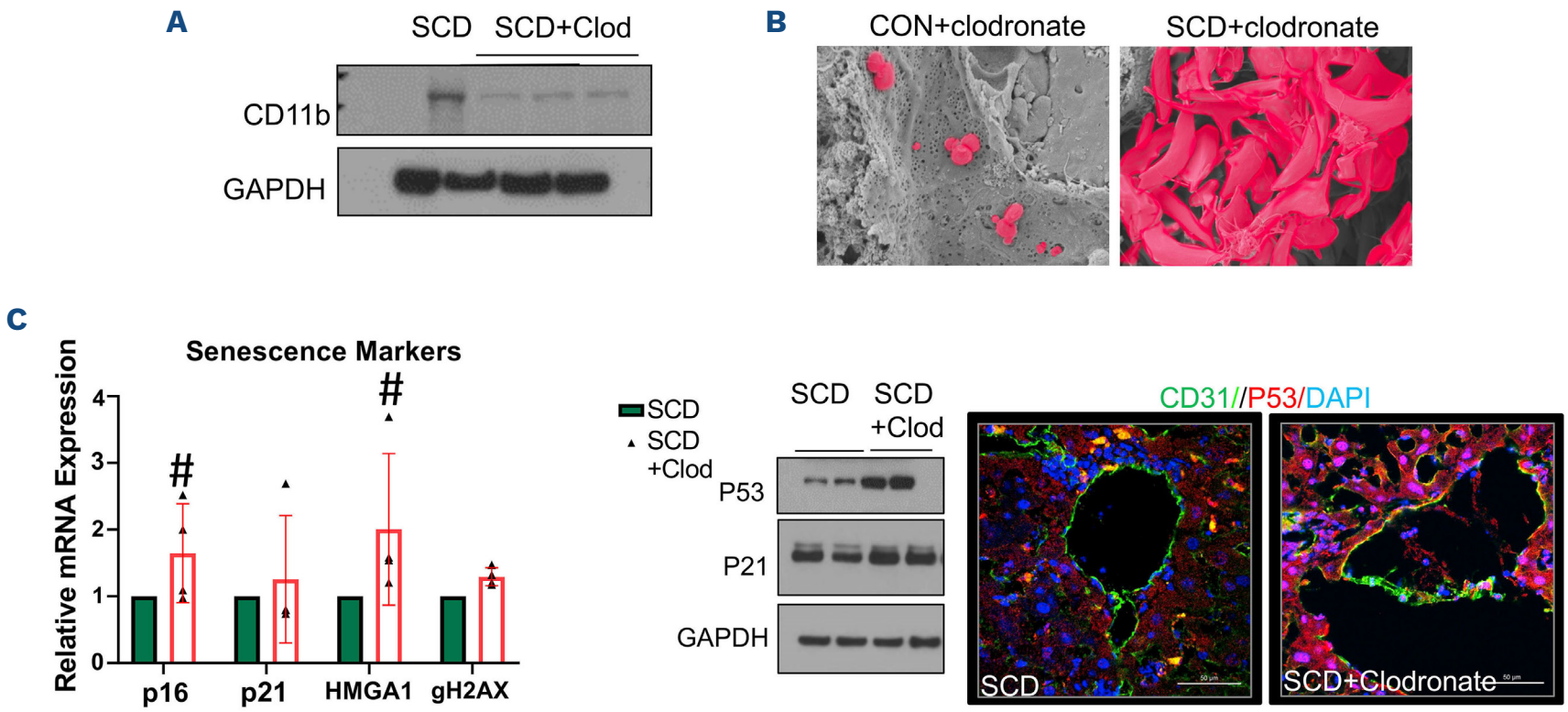

Continued on following page.

Figure 6. Loss of hepatic monocytes exacerbates liver sinusoidal endothelial cell senescence in sickle cell disease. (A) Western blot analysis of CD11b showing reduced expression in sickle cell disease (SCD) liver after clodronate-liposome treatment. (B) Representative scanning electron micrographs showing increased entrapment of erythrocytes in SCD liver after clodronate treatment. (C) Quantitative real-time polymerase chain reaction analysis of P21 and P16 shows increased expression in SCD liver after clodronate-liposome treatment. $^{\#}P$=0.04. Middle panel: western blot analysis of P21 and P53 showing increased expression in SCD liver after clodronate-liposome treatment. Right panel: representative immunofluorescence images displaying strong co-localization of CD31 and P53 in SCD liver after clodronate-liposome treatment compared with SCD liver at baseline. (D) Representative immunofluorescence images showing a strong increase in hemoglobin staining intensity in SCD liver tissue after clodronate treatment. Middle panel: western blot analysis of hemoglobin showing increased expression in SCD liver after clodronate-liposome treatment. Right panel: representative immunofluorescence images showing strong co-localization of hemoglobin and CD31 in SCD liver after clodronate-liposome treatment. (E) Representative images of tissues stained with hematoxylin and eosin show increased parenchymal injury in SCD liver after clodronate treatment compared to that in SCD liver alone (100X). Representative Sirius red (100X) and α-smooth muscle actin (100X) immunohistochemistry images demonstrate increased liver fibrosis in SCD+clodronate liver compared to SCD liver alone. (F) Representative quantitative liver intravital microscopy images of two different fields of view of SCD and clodronate-liposome-treated SCD liver injected with Texas red-dextran. Loss of blood flow (dark area devoid of red staining) is seen in SCD liver and is exacerbated in SCD liver treated with clodronate. Original magnification, ×10. Scale bar 50 μm. GAPDH: glyceraldehyde-3-phosphate dehydrogenase; Clod: clodronate; CON: control; DAPI: 4',6-diamidino-2-phenylindole; Hb: hemoglobnin; S. Red: Sirius red; α-SMA: alpha smooth muscle actin; H&E: hematoxylin and eosin; TXR: Texas red.

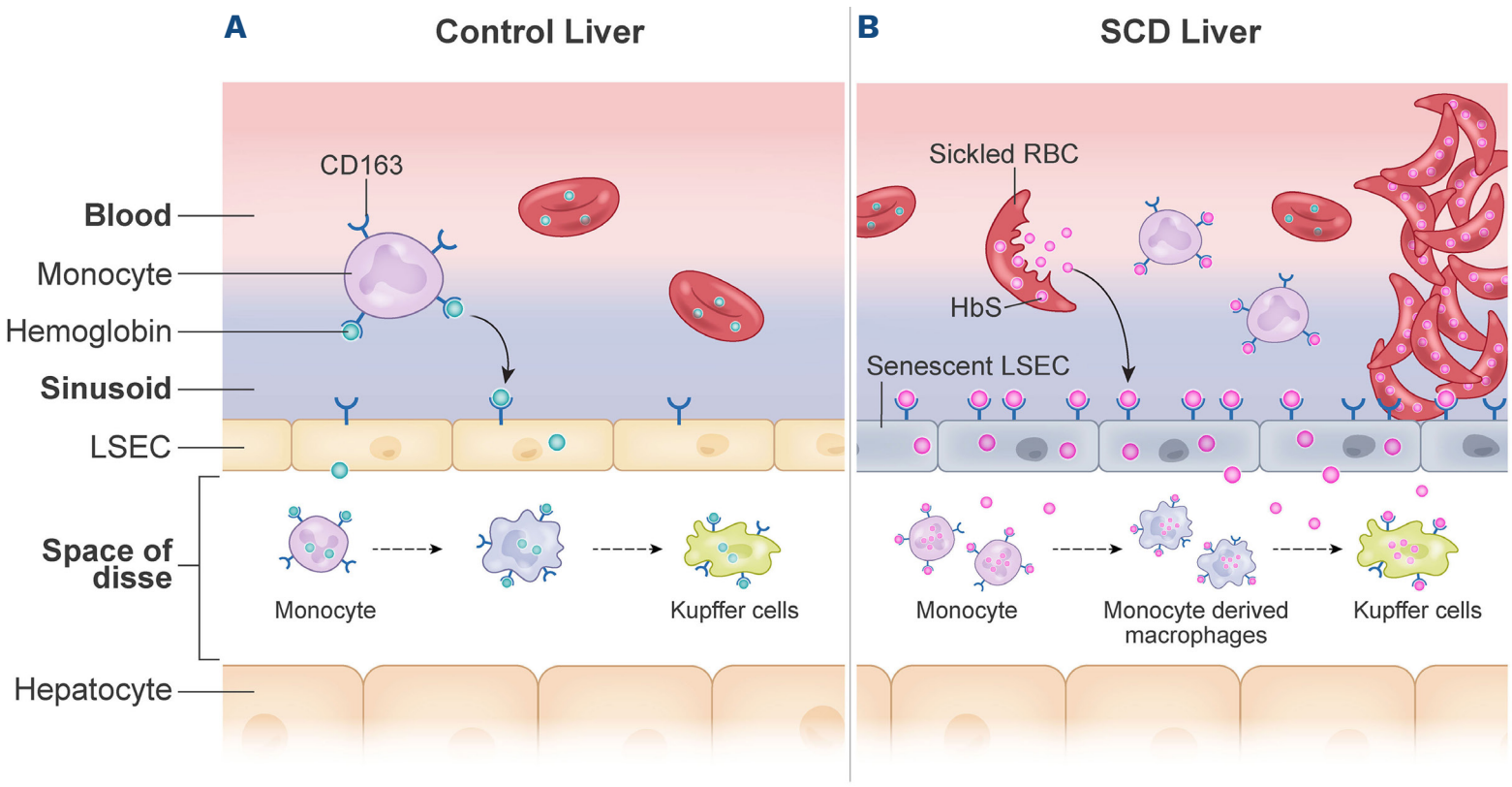

Figure 7. Impaired hemoglobin clearance by sinusoidal endothelium promotes vaso-occlusion and liver injury in sickle cell disease. Schematic diagram showing hemoglobin clearance in normal and sickle cell disease (SCD) liver. (A) In normal liver, the main cells responsible for hemoglobin clearance are hepatic Küpffer cells. Normal hemoglobin can also be endocytosed by liver sinusoidal endothelial cells (LSEC) and cleared without affecting LSEC viability. (B) In SCD liver, stressed, aged sickle erythrocytes accumulate in the hepatic sinusoids, where they are subsequently eliminated by hepatic leukocytes. Due to the continuous accumulation of sickle erythrocytes, their sequestration and hemolysis, hepatic macrophages and monocytes are activated to clear hemoglobin and iron released from these erythrocytes. LSEC participate actively in hepatic hemoglobin clearance in order to prevent the prolonged accumulation of hemoglobin and the associated tissue damage. Nonetheless, HbS/iron accumulation promotes LSEC senescence, resulting in delayed clearance, retention of HbS/iron, and increased liver injury. RBC: red blood cell.

Our findings suggest that the following sequence of events contributes to LSEC senescence in SCD mouse liver (Figure 7A, B). First, sickle erythrocytes are sequestered in hepatic sinusoids, thereby promoting hepatic ischemia followed by intravascular hemolysis. Second, hepatic macrophages and monocytes are activated to clear HbS, and iron released by the lysed erythrocytes, but the amount of HbS/iron released in SCD overwhelms the hepatic monocyte/macrophage-dependent clearance mechanism, leading to participation of LSEC in hepatic HbS/iron clearance through micropinocytosis. However, accumulation of HbS/iron in the LSEC leads to senescence of these cells, which in turn further promotes sinusoidal ischemia, liver injury and liver fibrosis. It will be interesting to examine whether non-SCD mouse models of other diseases characterized by intravascular hemolysis (e.g., thalassemia, sepsis) exhibit LSEC senescence.

Studies over the last few decades have focused on understanding the multifaceted pathophysiology associated with HbS polymerization and have led to the identification of

many new therapeutic targets in SCD, such as P-selectin. P-selectin is an adhesion molecule present on endothelial cells and platelets[48] which promotes erythrocyte-leukocyte-platelet-endothelial adhesion, leading to vaso-occlusion in SCD.[49,50] We[34] and others[16] have shown that monocytes recruited to the liver attenuate hepatic damage in SCD mice by promoting hemoglobin and iron recycling. Our current findings suggest that genetic deletion of P-selectin in SCD mice worsens liver injury by impairing hemoglobin and iron clearance in the liver, which is secondary to reduced recruitment of monocytes caused by the absence of P-selectin. Crizanlizumab, a humanized monoclonal P-selectin-blocking antibody, is the first targeted therapy approved by the US Food and Drug Administration for the prevention of vaso-occlusive pain episodes in SCD patients.[51] Although our current findings suggest that genetic (chronic) absence of P-selectin activity exacerbates liver injury in SCD mice, it remains to be determined whether chronic therapy with crizanlizumab might also increase the risk of liver injury in patients with SCD by promoting LSEC senescence. Unfortunately, biomarkers of liver injury were not reported in the paper on the crizanlizumab phase II clinical trial, and they are not routinely measured in clinical practice after crizanlizumab infusions. Thus, although no clinically significant liver injury has been reported after crizanlizumab treatment, it remains to be determined whether subtle alterations of liver indices may occur following P-selectin blockade in humans. Regardless of this limitation, our findings highlight the importance of monitoring liver function in patients on chronic crizanlizumab therapy.

Our study does have a few limitations that warrant further investigation in the future. First, the current study suggests that HbS is responsible for promoting senescence in LSEC by inducing a senescence-associated secretory phenotype (SASP) in the microenvironment; however, the cause-and-effect relationship between these pathological events and the signaling pathways affected remain to be elucidated. Second, we have shown that LSEC can promote hemoglobin clearance. However, it remains to be determined which scavenger receptor contributes specifically to HbS clearance by LSEC. Similarly, there are multiple micropinocytosis pathways of endocytic uptake, but which pathway promotes HbS uptake by LSEC in SCD and why LSEC are inefficient at degrading HbS remain to be determined. Notwithstanding these limitations, the current study is the first to show that LSEC promote hemoglobin clearance in SCD mouse liver and that HbS-induced LSEC senescence is associated with chronic liver injury in SCD. These findings suggest that attenuating LSEC senescence by using senolytics[52] or mitigating HbS/iron accumulation in LSEC could potentially ameliorate chronic liver injury in SCD.

Disclosures

HZ works at BioMagis. PS has received funds from CSL Behring, Novartis, and IHP Therapeutics. GJK works at CSL Behring. EMN is a consultant for Novo Nordisk and Chiesi. All other authors declare that they have no conflicts of interest to disclose.

Contributions

TWK, OK, ZL, RD, CH, AA, HZ, and TP-S conducted the experiments. HZ, TK, OK, and TP-S analyzed the data. GJK, TB, and PS provided important reagents or resources. TP-S wrote the manuscript with suggestions from and consultation with EM-N and PS.

Acknowledgments

The authors thank Pittsburgh Center for Biological Imaging (CBI-PITT), Dr. Donna Stolz, Dr. Simon Watkins, Dr. Jesus Tejero, Dr. Ramakrishna Ungalara, Jonathan Frank, Mara Sullivan, Laura Nelson, and X Zhang for their technical assistance in this study.

Funding

This work was supported by National Institutes of Health (NIH), National Institute of Diabetes and Digestive and Kidney Diseases grant K01NIH-NIDDK125617, an American Society of Hematology Junior Faculty Scholar Award (to TP-S), NIH, National Heart, Lung, and Blood Institute grants R01HL128297 and R01HL141080 (to PS); American Heart Association (AHA) grant 18TPA34170588 (to PS); and an AHA postdoctoral fellowship AHA828786 (to TWK).

Data-sharing statement

All data related to this study are shared through this manuscript. For further information please contact the corresponding author.

References

1. Sundd P, Gladwin MT, Novelli EM. Pathophysiology of sickle cell disease. Annu Rev Pathol. 2019;14:263-292.
2. Wang Q, Zennadi R. The role of RBC oxidative stress in sickle cell disease: from the molecular basis to pathologic implications. Antioxidants (Basel). 2021;10(10):1608.
3. Lacaille F, Allali S, Montalembert M De. The liver in sickle cell disease. J Pediatr Gastroenterol Nutr. 2021;23(2):177-189.
4. Kyrana E, Rees D, Lacaille F, et al. Clinical management of sickle cell liver disease in children and young adults. Arch Dis Child. 2020;106(4):315-320.
5. Ross AS, Graeme-Cook F, Cosimi AB, et al. Combined liver and kidney transplantation in a patient with sickle cell disease. Transplantation. 2002;73(4):605-608.
6. Galloway-Blake K, Reid M, Walters C, et al. Clinical factors associated with morbidity and mortality in patients admitted with sickle cell disease. West Indian Med J. 2014;63(7):711-716.

7. Ware RE, de Montalembert M, Tshilolo L, et al. Sickle cell disease. Lancet. 2017;390(10091):311-323.
8. George A, Pushkaran S, Konstantinidis DG, et al. Erythrocyte NADPH oxidase activity modulated by Rac GTPases, PKC, and plasma cytokines contributes to oxidative stress in sickle cell disease. Blood. 2013;121(11);2099-2107.
9. Franco RS, Lohmann J, Silberstein EB, et al. Time-dependent changes in the density and hemoglobin F content of biotin-labeled sickle cells. J Clin Invest. 1998;101(12):2730-2740.
10. Lutz HU, Bogdanova A. Mechanisms tagging senescent red blood cells for clearance in healthy humans. Front Physiol. 2013;4:387.
11. Lee SJ, Park SY, Jung MY, et al. Mechanism for phosphatidylserine-dependent erythrophagocytosis in mouse liver. Blood. 2011;117(19):5215-5223.
12. Thomsen JH, Etzerodt A, Svendsen P, et al. The haptoglobin-CD163-heme oxygenase-1 pathway for hemoglobin scavenging. Oxid Med Cell Longev. 2013;2013:523652.
13. Pradhan-Sundd T, Vats R, Russell JO, et al. Dysregulated bile transporters and impaired tight junctions during chronic liver injury in mice. Gastroenterology. 2018;155(4):1218-1232.
14. Wu LC, Sun CW, Ryan TM, et al. Correction of sickle cell disease by homologous recombination in embryonic stem cells. Blood. 2006;108(4):1183-1188.
15. Vats R, Brzoska T, Bennewitz MF, et al. Platelet extracellular vesicles drive inflammasome-IL-1β-dependent lung injury in sickle cell disease. Am J Respir Crit Care Med. 2020;201(1):33-46.
16. Liu Y, Zhong H, Bao W, et al. Patrolling monocytes scavenge endothelial adherent sickle red blood cells in sickle cell disease. Blood. 2018;134(7):579-590.
17. Pradhan-Sundd T, Kato GJ, Novelli EM. Molecular mechanisms of hepatic dysfunction in sickle cell disease: lessons from Townes mouse model. Am J Physiol Cell Physiol. 2022;323(2):C494-C504.
18. Bennewitz MF, Tutuncuoglu E, Gudapati S, et al. P-selectin-deficient mice to study pathophysiology of sickle cell disease. Blood Adv. 2020;4(2):266-273.
19. Vats R, Liu S, Zhu J, et al. Impaired bile secretion promotes hepatobiliary injury in sickle cell disease. Hepatology. 2020;72(6):2165-2181.
20. Anzinger JJ, Chang J, Xu Q, et al. Native low-density lipoprotein uptake by macrophage colony-stimulating factor-differentiated human macrophages is mediated by macropinocytosis and micropinocytosis. Arterioscler Thromb Vasc Biol. 2010;30(10):2022-2031.
21. Braet F, De Zanger R, Jans D, et al. Microfilament-disrupting agent latrunculin A induces an increased number of fenestrae in rat liver sinusoidal endothelial cells: comparison with cytochalasin B. Hepatology. 1996;24(3):627-635.
22. Vats R, Kaminski TW, Pradhan-Sundd T. Intravital imaging of hepatic blood biliary barrier in live mice. Curr Prot. 2021;1(10):e256.
23. Racanelli V, Rehermann B. The liver as an immunological organ. Hepatology. 2006;43(2 Suppl 1):S54-62.
24. Elvevold K, Kyrrestad I, Smedsrød B. Protocol for isolation and culture of mouse hepatocytes (HCs), Kupffer cells (KCs), and liver sinusoidal endothelial cells (LSEC) in analyses of hepatic drug distribution. Methods Mol Biol. 2012;2434:385-402.
25. Theurl I, Hilgendorf I, Nairz M, et al. On-demand erythrocyte disposal and iron recycling requires transient macrophages in the liver. Nat Med. 2016;22(8):945-951.
26. Chang R, Castillo J, Zambon AC, et al. Brain endothelial erythrophagocytosis and hemoglobin transmigration across brain endothelium: implications for pathogenesis of cerebral microbleeds. Front Cell Neurosci. 2018;12:279.
27. Fens MHAM, van Wijk R, Andringa G, et al. A role for activated endothelial cells in red blood cell clearance: implications for vasopathology. Haematologica. 2012;97(4):500-508.
28. Oh N, Park JH. Endocytosis and exocytosis of nanoparticles in mammalian cells. Int J Nanomedicine. 2014;9(Suppl 1):51-63.
29. Cao H, Chen J, Awoniyi M, et al. Dynamin 2 mediates fluid-phase micropinocytosis in epithelial cells. J Cell Sci. 2007;120(Pt23):4167-4177.
30. Richards DA, Rizzoli SO, Betz WJ. Effects of wortmannin and latrunculin A on slow endocytosis at the frog neuromuscular junction. J Physiol. 2004;557(Pt 1):77-91.
31. Browne P, Shalev O, Hebbel RP. The molecular pathobiology of cell membrane iron: the sickle red cell as a model. Free Radic Biol Med. 1998;24(6):1040-1048.
32. Klei TRL, Meinderts SM, van den Berg TK, et al. From the cradle to the grave: the role of macrophages in erythropoiesis and erythrophagocytosis. Front Immunol. 2017;8:73.
33. Vinchi F, Da Silva MC, Ingoglia G, et al. Hemopexin therapy reverts heme-induced proinflammatory phenotypic switching of macrophages in a mouse model of sickle cell disease. Blood. 2016;127(4):473-486.
34. Vats R, Kaminski TW, Ju E-M, et al. P-selectin deficiency promotes liver senescence in sickle cell disease mice. Blood. 2021;137(19):2676-2680.
35. Liu Y, Zhong H, Bao W, et al. Patrolling monocytes scavenge endothelial-adherent sickle RBCs: a novel mechanism of inhibition of vaso-occlusion in SCD. Blood. 2019;134(7):579-590.
36. Biburger M, Aschermann S, Schwab I, et al. Monocyte subsets responsible for immunoglobulin G-dependent effector functions in vivo. Immunity. 2011;35(6):932-944.
37. George A, Conneely SE, Mangum R, et al. Splenic complications in sickle cell disease: a retrospective cohort review. Blood. 2021;108(4):1158-1162.
38. Terpstra V, Van Berkel TJC. Scavenger receptors on liver Kupffer cells mediate the in vivo uptake of oxidatively damaged red blood cells in mice. Blood. 2000;95(6):2157-2163.
39. Schaer DJ, Schaer CA, Buehler PW, et al. CD163 is the macrophage scavenger receptor for native and chemically modified hemoglobins in the absence of haptoglobin. Blood. 2006;107(1):373-380.
40. Gbotosho OT, Kapetanaki MG, Kato GJ. The worst things in life are free: the role of free heme in sickle cell disease. Front Immunol. 2021;11:561917.
41. Santiago RP, Guarda CC, Figueiredo CVB, et al. Serum haptoglobin and hemopexin levels are depleted in pediatric sickle cell disease patients. Blood Cells Mol Dis. 2018;72:34-36.
42. Sundd P, Gladwin MT, Novelli EM. Pathophysiology of sickle cell disease. Ann Rev Pathol. 2019;14:263-292.
43. Ghosh S, Adisa OA, Chappa P, et al. Extracellular hemin crisis triggers acute chest syndrome in sickle mice. J Clin Invest. 2013;123(11):4809-4820.
44. Belcher JD, Chen C, Nguyen J, et al. Heme triggers TLR4 signaling leading to endothelial cell activation and vaso-occlusion in murine sickle cell disease. Blood. 2014;123(3):377-390.
45. Kuilman T, Michaloglou C, Mooi WJ, et al. The essence of senescence. Genes Dev. 2010;24(22):2463-2479.
46. Hutchins NA, Chung CS, Borgerding JN, et al. Kupffer cells protect liver sinusoidal endothelial cells from Fas-dependent apoptosis in sepsis by down-regulating gp130. Am J Pathol. 2013;182(3):742-754.
47. Koudelkova P, Weber G, Mikulits W. Liver sinusoidal endothelial

cells escape senescence by loss of p19ARF. PLoS One. 2015;10(11):e0142134.
48. Matsui NM, Borsig L, Rosen SD, et al. P-selectin mediates the adhesion of sickle erythrocytes to the endothelium. Blood. 2001;98(6):1955-1962.
49. Vats R, Tutuncuoglu E, Pradhan-Sundd T, et al. Tandem P-selectin glycoprotein ligand immunoglobulin prevents lung vaso-occlusion in sickle cell disease mice. Exp Hematol. 2020;84:1-6.
50. Vats R, Li Z, Ju EM, et al. Intravital imaging reveals inflammation as a dominant pathophysiology of age-related hepatovascular changes. Am J Physiol Cell Physiol. 2022;322(3):C508-C520.
51. Ataga KI, Kutlar A, Kanter J, et al. Crizanlizumab for the prevention of pain crises in sickle cell disease. N Engl J Med. 2017;376(5):429-439.
52. Kirkland JL, Tchkonia T. Senolytic drugs: from discovery to translation. J Int Med. 2020;288(5):518-536.